ACS SENSORS

pubs.acs.org/acssensors

Letter

Ultrasensitive and Label-Free Detection of the Measles Virus Using an N-Heterocyclic Carbene-Based Electrochemical Biosensor

Robert M. Mayall, Christene A. Smith, Alexander S. Hyla, Dianne S. Lee, Cathleen M. Crudden,* and Viola I. Birss*

Cite This: *ACS Sens.* 2020, 5, 2747−2752

Read Online

ACCESS | Metrics & More | Article Recommendations | Supporting Information

ABSTRACT: With the current intense need for rapid and accurate detection of viruses due to COVID-19, we report on a platform technology that is well suited for this purpose, using intact measles virus for a demonstration. Cases of infection due to the measles virus are rapidly increasing, yet current diagnostic tools used to monitor for the virus rely on slow (>1 h) technologies. Here, we demonstrate the first biosensor capable of detecting the measles virus in minutes with no preprocessing steps. The key sensing element is an electrode coated with a self-assembled monolayer containing the measles antibody, immobilized through an N-heterocyclic carbene (NHC). The intact virus is detected by changes in resistance, giving a linear response to 10−100 μg/mL of the intact measles virus without the need to label or process the sample. The limit of detection is 6 μg/mL, which is at the lower limit of concentrations that can cause infections in primates. The NHC-based biosensors are shown to be superior to thiol-based systems, producing an approximately 10× larger response and significantly greater stability toward repeated measurements and long-term storage. This NHC-based biosensor thus represents an important development for both the rapid detection of the measles virus and as a platform technology for the detection of other biological targets of interest.

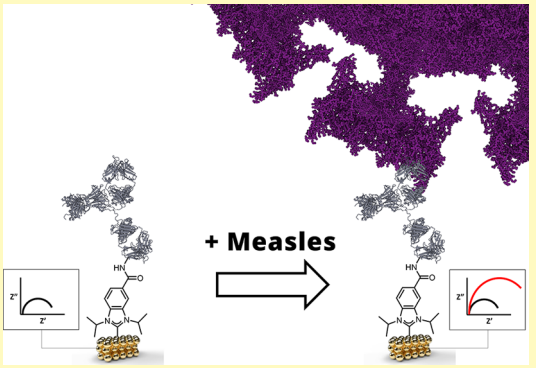

KEYWORDS: *biosensor, electrochemistry, viral detection, N-heterocyclic carbene, self-assembled monolayers*

Despite the widespread availability of a vaccine for measles, infections from the measles virus increased by over 300% in the first quarter of 2019,[1] likely a consequence of its high basic reproduction number (R_0 = 12−18).[2] This value is significantly higher than for other viruses of large-scale public health concern, including the SARS-CoV-2 coronavirus (R_0 = 1.4−3.9)[3] and smallpox (R_0 = 3.5−6).[4] Rapid identification and quarantine protocols are hampered by current detection methodologies, which are relatively slow (>1 h).[5] While polymerase chain reactions are the World Health Organization-recommended method, some laboratories, especially in the developing world, rely on simpler immunological methods, requiring hours to days for detection. Thus, there is an urgent need for a rapid and sensitive method to detect the measles virus to prevent the rapid spread of the disease. While biosensors have been previously explored for the detection of measles,[6,7] these efforts have involved detection of the human immune response after the disease has taken hold, rather than identification of the virus itself before symptoms appear.

Here, we describe an ultrasensitive method for the rapid detection of the measles virus using an antibody (Ab)-based electrochemical sensor. The antibody is attached to an Au electrode via a self-assembled monolayer (SAM) based on N-heterocyclic carbenes (NHCs). Although most common SAMs used in electrochemical sensors are thiol-based,[8] these are known to suffer from instability, leading to irreproducibility.[9] Recently, NHCs have been shown to form more robust SAMs that can be tethered to a range of metal surfaces, with exemplary resistance to degradation.[10,11] However, to date, NHC-based biosensors have only been described using optical techniques, such as surface plasmon resonance.[12−14] In this work, we employ an antibody (Ab) that is specific toward the transmembrane H protein of the measles virus.[15] Thus, we require no preprocessing steps to break open the virus particles prior to sensing (i.e., viral lysis), providing a simpler workflow compared to current approaches.[5] The resulting sensors have a linear response to 10−100 μg/mL of the intact measles virus, with a limit of detection of 6 μg/mL, encompassing the range of virus concentrations relevant to human health applications. A gamma-inactivated virus was used in this work, preserving the properties of the viral capsid such that it is comparable to live virions,

Received: June 21, 2020
Accepted: August 21, 2020
Published: August 21, 2020

Scheme 1. Assembly of Ab-SAM Electrochemical Measles Virus Sensor and Fc−SAM Model[a]

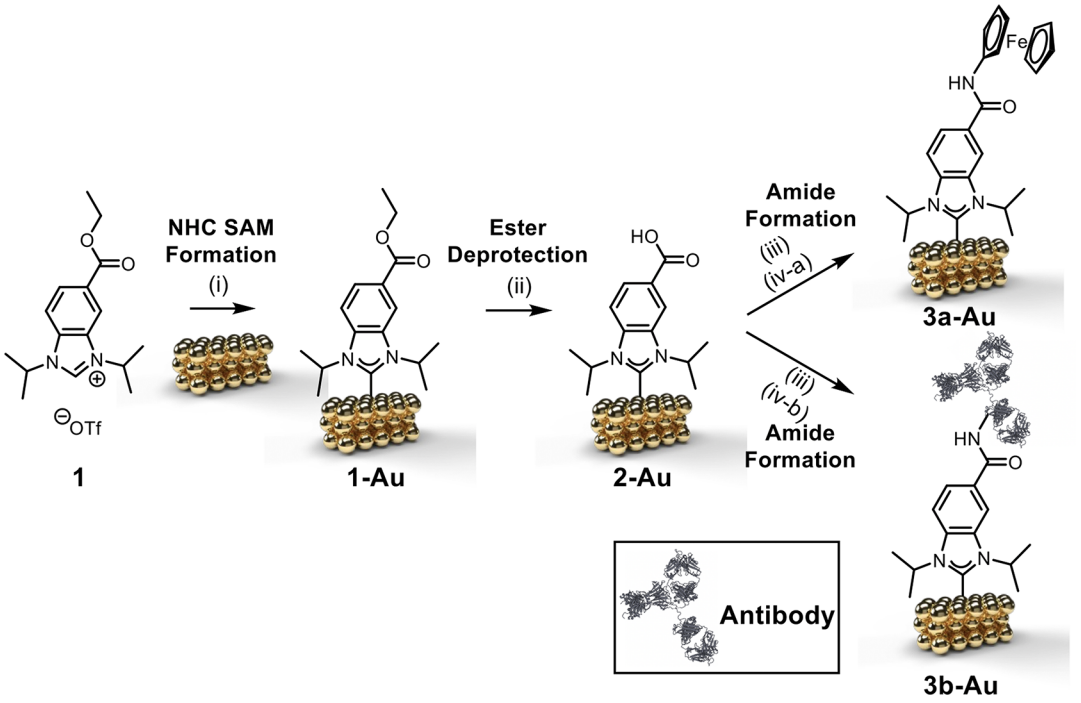

[a](i) 2 equiv $KHCO_3$ in MeOH, 24 h, RT. (ii) 2000 equiv KOH in EtOH, 24 h, RT. (iii) 2 mM EDC, 9.5 mM NHS, 0.11 M MES in water, 1 h, RT. (iv-a) 1 mM $FcNH_2$ in water, 24 h, 4 °C and (iv-b) 1 μg/mL Ab, 24 h, 4 °C. Ab = Antibody, SAM = self−assembled monolayer, Fc = ferrocene.

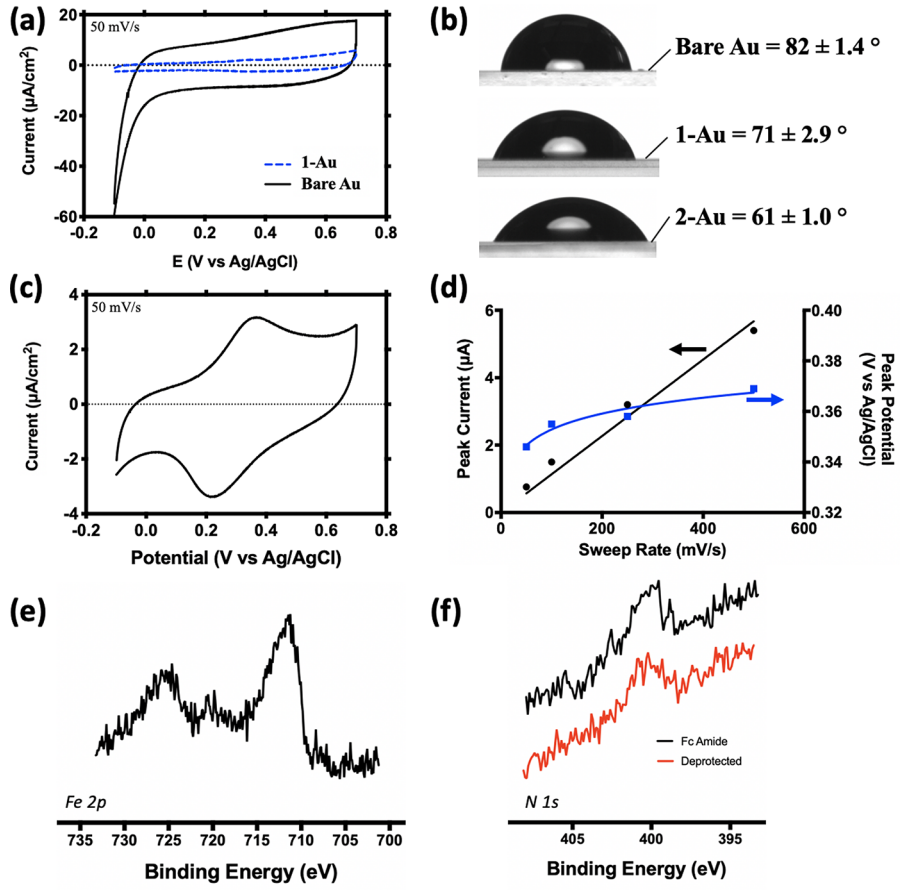

Figure 1. (a) CV of bare Au and **1-Au** ester-NHC SAM in 1 M $NaClO_4$, (b) Contact angles for bare Au and **1-Au** and **2-Au** SAMs, (c) CV and (d) peak characteristics of Fc-NHC SAM, (e,f) XPS showing Fe 2p and N 1s regions for the Fc-NHC and COOH-terminated SAMs.

https://dx.doi.org/10.1021/acssensors.0c01250
ACS Sens. 2020, 5, 2747−2752

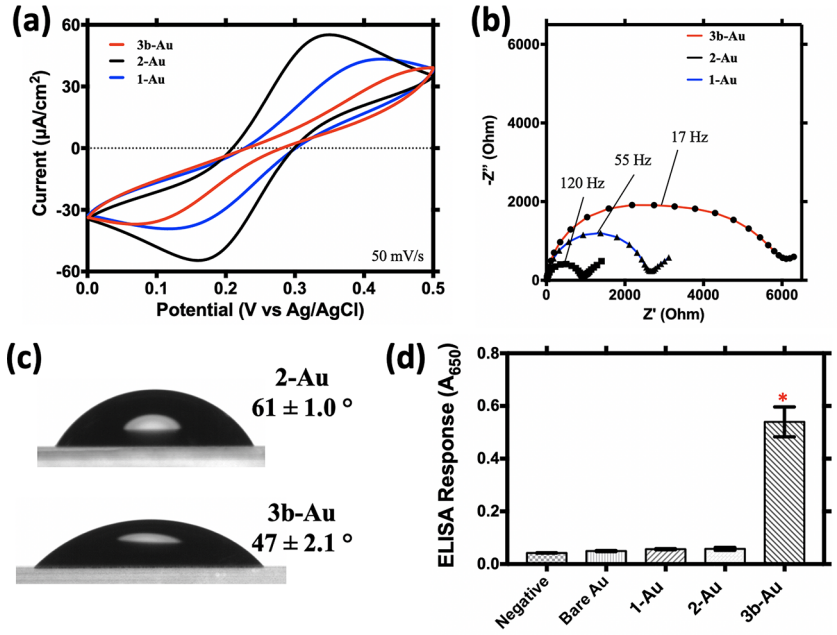

Figure 2. (a) CV and (b) impedance spectroscopy in 5 mM ferro/ferricyanide. (c) Contact angle and (d) ELISA results for the measles sensor, before and after Ab immobilization on the modified SAM.

including those found in aerosols. This approach is thus expected to have a significant impact on measles monitoring and could be generalized to other viruses, including SARS-CoV-2.

To fabricate the biosensor (Scheme 1), we prepared a previously described ethyl ester-terminated benzimidazolium trifluoromethanesulfonate salt **1** (Scheme 1).[16] The SAM was formed by placing clean Au into a methanolic solution of **1** and $KHCO_3$ for 24 h, followed by thorough washing, affording the ester-NHC SAM **1-Au**. The drop in the double layer charging current of the Au electrode after ester-NHC SAM formation observed by cyclic voltammetry (CV) confirms the deposition of an insulating layer (Figure 1a).[17] Contact angle analysis (Figure 1b) provided further evidence for SAM formation, as the surface hydrophilicity increased after ester-NHC deposition. It should be noted that, due to a lower degree of surface ordering, contact angles for NHC SAMs are typically lower than those of comparable thiol SAMs.[10]

Hydrolysis of the ester with base forms a carboxyl-terminated monolayer, **2-Au**. The success of this step was also confirmed by contact angle measurements, which showed a decrease in contact angle after ester hydrolysis, consistent with the more hydrophilic carboxylic acid-terminated surface (Figure 1b).

The presence of the carboxylic acid on the surface was further confirmed by its reactivity in amide coupling reactions. Using a standard amide coupling protocol with EDC, NHS, and MES,[18] aminoferrocene ($FcNH_2$) was reacted with the SAM for 24 h at 4 °C to form **3a-Au**. Ferrocene was employed due to its ability to be easily observed electrochemically and via XPS, as well as its use in biosensor designs.[19] The coupling was carried out at a low temperature to mimic the conditions that would be necessary for the attachment of the measles Ab.

Following amide coupling, Fc redox peaks were seen at 0.25 V (cathodic) and 0.35 V (anodic) (Figure 1c). The classical sweep rate dependence of the electroactive surface species (Figure 1d) confirms that the Fc-NHC redox chemistry is very rapid, as expected.[20] It was shown from electrochemical and computational data in prior published work that one full monolayer of an NHC SAM equates to 3.5 molecules/cm^2.[10] As our calculated Fc surface density is 0.88 molecules/nm^2, this corresponds to ~25% of a single NHC monolayer.[10] Assuming that the Fc surface density reflects the NHC SAM surface coverage, this is more than sufficient to form a full monolayer of the immobilized anti-measles antibody in **3b-Au**, due to the much larger size of proteins (>1 nm^2) compared to the NHC molecules (~0.3 nm^2).[10]

XPS analysis of the surface after amide bond formation with aminoferrocene shows the presence of Fe^{2+}. The observed N:Fe ratio of approximately 3:1 is consistent with the full conversion of the ester-NHC SAM to the Fc-NHC SAM (Figure 1e,f). However, due to the fact that NHC SAMs are still relatively unexplored and have never been previously modified with EDC/NHS while attached to a Au surface, DFT analysis was carried out to confirm that the Au-NHC bond would remain stable. Figures S2−3 and Table S1 suggest that each stage (**1-Au**, **2-Au**, and **3a-Au**) has a similar reorganization of charge density at the Au/NHC interface, with no significant differences arising from the amide coupling procedure. The DFT analysis also predicted fast electron transfer between the NHC and Au, critical to rapid sensor response. Figure 1 and the DFT results thus provide a strong indication that the NHC-SAMs will be stable and can be further modified after deposition on Au.

Having demonstrated that the carboxylic acid-terminated NHC is a suitable surface for coupling to simple amines such as $FcNH_2$, we employed these conditions to bind the anti-measles Ab to the SAM. The effectiveness of this step was confirmed by electrochemical measurements, contact angle analysis, and a modified enzyme-linked immunosorbent assay (ELISA).[19] Both CVs (Figure 2a) and impedance (Figure 2b) clearly show that the Ab was successfully immobilized on the NHC surface (**3b-Au**), as the CV peak separation increases, the peak current decreases, and the impedance increases (Tables S2,3).

Contact angle analysis (Figure 2c) demonstrates that the sensor surface becomes more hydrophilic after modification by the measles Ab, as expected. Finally, the ELISA response of the various surfaces clearly demonstrates the immobilization of the measles Ab. Figure 2d clearly shows that only the final surface

https://dx.doi.org/10.1021/acssensors.0c01250
ACS Sens. 2020, 5, 2747−2752

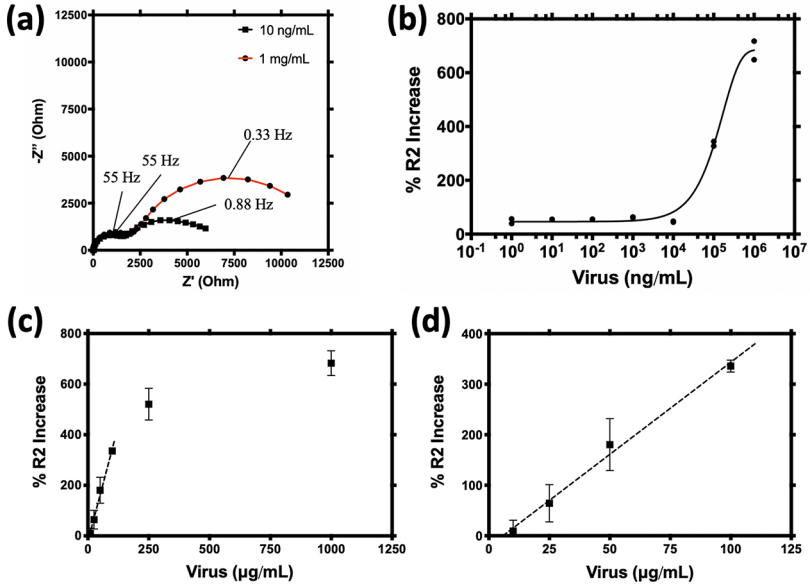

Figure 3. (a) Nyquist plot of **3b-Au** in 5 mM ferro/ferricyanide with low and high measles concentrations. % Change of R2 over a (b) large and (c,d) narrow range of measles concentrations.

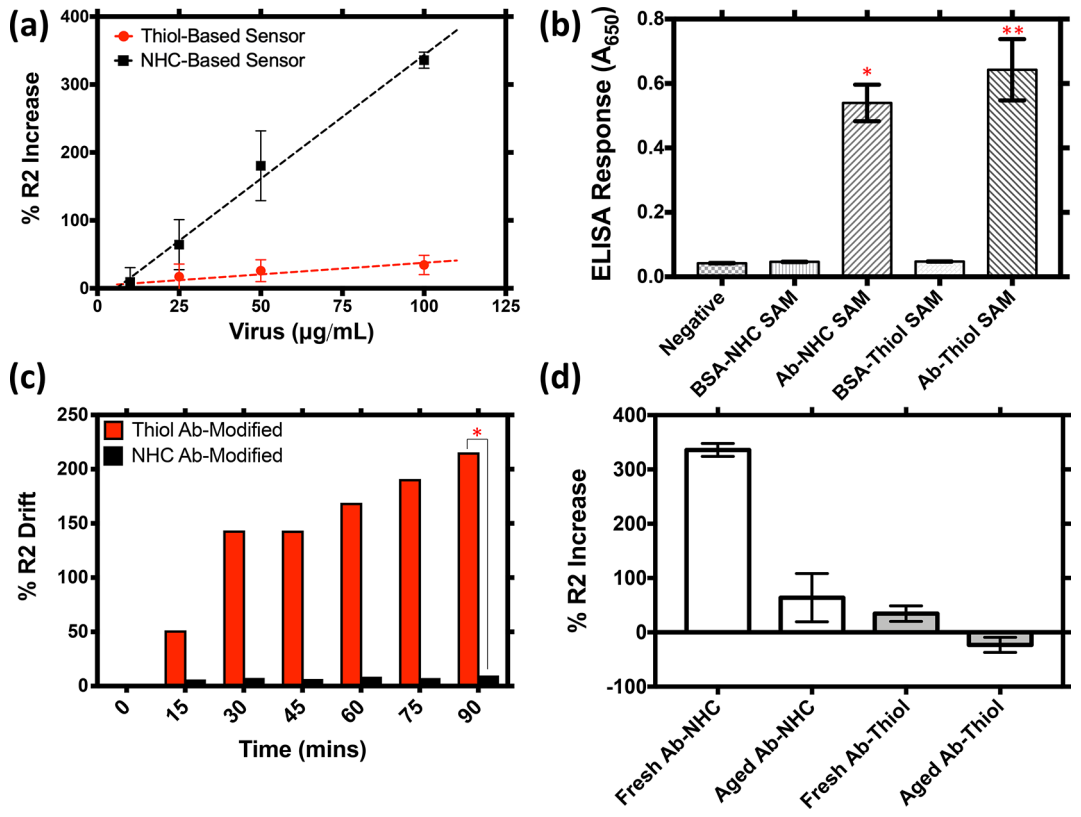

Figure 4. (a) Resistance increase of NHC and thiol Ab-SAM sensors to measles virus concentration ($n = 3$). (b) ELISA response from sensors modified with Ab or BSA ($n = 9$). (c) Change in R2 over repeated measurements. (d) Response to 100 μg/mL of measles virus before (Fresh) and after 2 weeks of storage at 4 °C (Aged), $n = 3$.

resulting from NHC SAM formation, ester hydrolysis, and coupling with the measles Ab has a response above background ($p < 0.005$). This response, quantified by measuring the absorbance at 650 nm as the ELISA substrate (TMB) is oxidized by the horseradish peroxidase-labeled secondary Ab, indicates that this secondary Ab was bound to the modified SAM and verifies that the anti-measles Ab was successfully immobilized on the NHC SAM surface.

With anti-measles Ab-functionalized electrodes in hand, we then examined the response (in 5 mM ferro/ferricyanide) of the Ab-modified electrodes to various concentrations of gamma-inactivated measles virus without labeling or preprocessing (i.e., lysis). The Nyquist plot shown in Figure 3a demonstrates that,

https://dx.doi.org/10.1021/acssensors.0c01250
ACS Sens. 2020, 5, 2747−2752

from 1 ng/mL to 1 mg/mL, the high-frequency arc experienced little change, as it originates from the underlying SAM (Figure S5), while the low-frequency resistance changed substantially (Figure 3a, Table S4) for two duplicate biosensors.

The sigmoidal R2/concentration curve in Figure 3b is the classical response expected from an antibody interacting with its target, with no binding (low % increase) observed until 10 μg/mL of the intact virion is present and a plateau seen above 1 mg/mL of measles virus. The sensors demonstrated exceptional reproducibility, with minimal variation until the sensor response was saturated. The EC_{50}, a measure of the strength of an interaction between an Ab and target molecule, was 118 μg/mL (R^2 = 0.990) for the immobilized Ab and the measles virus.

A reproducible linear response is shown in Figure 3c,d for triplicate NHC SAM biosensors over a narrow range of measles virus concentrations (1 μg/mL to 1 mg/mL), giving a limit of detection of 6 μg/mL (R^2 = 0.957). The sensor response plateaus at higher concentrations, with a minimal increase above 250 μg/mL of the virus. The infectious dose for the measles virus, based on primate studies, is 10^6−10^8 virus particles.[21,22] Using electron microscopy data,[23] this converts to a minimum infectious dose of 1−100 μg/mL, which corresponds extremely well with the sensing range of the NHC-based measles biosensor described herein (Figure 3d). The 6 μg/mL limit of detection thus falls below the previously published infectious dose (ID_{50}) values. As the structure of the viral capsid was preserved in this work, the results from these experiments could be directly translated to aerosol detection of infectious measles virus.

To compare the NHC sensor platform performance with that obtained using traditional thiol-based monolayers, 6-mercaptohexanoic acid was employed to form a thiol-based SAM and the anti-measles antibody was tethered to it, using the amide coupling process described above. No defects were purposefully introduced into the thiol-based monolayer to emulate the 25% coverage observed in the case of the NHC-based SAMs. This is because thiol-based SAM stability relies more heavily on lateral interactions than is predicted for NHC-based SAMs.[10] Thus, a comparison of the stability of a thiol vs NHC-based SAM, both with a 25% coverage, would not be meaningful.

The electrochemical results (Figure S6, Table S5) showed that the thiol sensor produced a 10-fold smaller response to virus concentration (Figure 4a, S7), with a maximum increase in R2 of 60% at 1 mg/mL, compared to ∼650% for the NHC-based SAM. This is attributed to the lower packing density of NHC SAMs compared with thiolate SAMs,[10] resulting in a smaller proportional resistance increase upon binding of the virus.

In Figure 4b, we compare ELISA results for the thiol and NHC SAMs, where either bovine serum albumin (BSA, a negative control) or the anti-measles Ab were attached using the amide coupling procedure. A much larger response is obtained from both Ab-modified SAMs than for the BSA-modified or negative control samples, verifying that the antibody is tethered to these SAMs. The slightly higher ELISA signal for the Ab-modified thiol vs NHC-SAMs is likely indicative of the larger amount of Ab immobilized on the thiol-SAM. The response from the BSA samples is indistinguishable from the negative control (p < 0.0001), confirming that the ELISA response cannot be attributed to nonspecific binding.

Importantly, when BSA-thiol and BSA-NHC SAMs were tested with the measles virus, the sensor resistance did not change (Figure S8, Table S6). In addition, the thiol and NHC-based monolayers, both modified with the anti-measles Ab, were repeatedly tested using EIS over 90 min to establish their stability during the testing protocol. Figure 4c shows a much larger change in R2 for the thiol vs NHC-based monolayers, also seen by CV (Figure S9), indicating that the thiol-based monolayer was significantly less stable than the NHC SAM.

The differences in shelf life between the thiol and NHC-based sensors were also examined. In Figure 4d, we show the response of triplicate thiol and NHC-based sensors to 100 μg/mL of the measles virus directly after sensor construction ("Fresh") or after 2 weeks of storage at the Ab supplier's recommended temperature (4 °C, "Aged"). The response of both sensors after 2 weeks was much weaker, indicating degradation in both cases. However, the NHC-based sensors still responded to the virus after 2 weeks at 4 °C, albeit to a lesser degree than freshly prepared sensors (Figure 4d). Aged thiol-based sensors did not respond when challenged with the virus.

Considering the relative instability of proteins, which is exaccerbated in the presence of perchlorate,[24] it is plausible that the decrease in performance after the storage is due to protein degradation rather than loss of the SAM. However, the clear difference between the NHC and thiol SAMs cannot be attributed to Ab degradation alone. Thus, while aging issues need to be addressed, the NHC SAMs remain more stable than their thiol SAM counterparts.

In conclusion, we have developed an electrochemical biosensor for the intact measles virus using NHC SAMs. The NHC-based sensor produced a >10 times larger response to the virus than a comparable, conventional thiol-based sensor and also showed demonstrably greater stability. The sensor, which is active over the range of virus concentrations relevant to human health applications (6−100 μg/mL), is shown to function with the intact measles virus without the need for preprocessing (i.e., lysis) or labeling steps. Such a system could be directly translated to real-world detection, including monitoring aerosols for active viruses. Additionally, this sensor required ca. 15 min to perform the detection and has an estimated cost of only $3.72 USD per test (Tables S7,8), which would further aid in future implementation. While still preliminary, these results show great promise for the application of NHC SAMs in future electrochemical biosensors, both for the detection of the measles virus and as a platform technology for the detection of other biological targets of interest, including SARS-CoV-2.

■ ASSOCIATED CONTENT

Supporting Information

The Supporting Information is available free of charge at https://pubs.acs.org/doi/10.1021/acssensors.0c01250.

Experimental methods, supporting figures and tables (PDF)

■ AUTHOR INFORMATION

Corresponding Authors

Viola I. Birss − *Department of Chemistry, University of Calgary, Calgary, Alberta T2N 1N4, Canada*; Phone: 1-403-220-6432; Email: birss@ucalgary.ca

Cathleen M. Crudden − *Department of Chemistry, Queen's University, Kingston, Ontario K7L 3N6, Canada*; orcid.org/0000-0003-2154-8107; Email: cruddenc@chem.queensu.ca

Authors

Robert M. Mayall − *Department of Chemistry, University of Calgary, Calgary, Alberta T2N 1N4, Canada*; orcid.org/0000-0003-3197-2972

https://dx.doi.org/10.1021/acssensors.0c01250
ACS Sens. 2020, 5, 2747−2752

Christene A. Smith − *Department of Chemistry, Queen's University, Kingston, Ontario K7L 3N6, Canada;* orcid.org/0000-0003-2631-5783
Alexander S. Hyla − *Department of Chemistry, University of Calgary, Calgary, Alberta T2N 1N4, Canada*
Dianne S. Lee − *Department of Chemistry, Queen's University, Kingston, Ontario K7L 3N6, Canada*

Complete contact information is available at: https://pubs.acs.org/10.1021/acssensors.0c01250

Notes

The authors declare no competing financial interest.

■ ACKNOWLEDGMENTS

V.I.B. and C.M.C. acknowledge the Natural Sciences and Engineering Research Council of Canada (NSERC) and the Canada Foundation for Innovation (CFI) for financial support. R.M.M. would like to acknowledge Vanier Canada Graduate and Alberta Innovates Graduate Student scholarship support, C.A.S. would like to thank NSERC, and A.S.H. would like to thank the Canada First Research Excellence Fund for financial support. C.A.S. and D.S.L. would also like to thank Gabriele Schatte and Ishwar Singh for assistance with XPS.

■ REFERENCES

(1) Mahase, E. Measles Cases Rise 300% Globally in First Few Months of 2019. *BMJ.* **2019**, *365*, l1810.
(2) Guerra, F. M.; Bolotin, S.; Lim, G.; Heffernan, J.; Deeks, S. L.; Li, Y.; Crowcroft, N. S. The Basic Reproduction Number (R0) of Measles: A Systematic Review. *Lancet Infect. Dis.* **2017**, *17* (12), e420−e428.
(3) Li, Q.; Guan, X.; Wu, P.; Wang, X.; Zhou, L.; Tong, Y.; Ren, R.; Leung, K. S. M.; Lau, E. H. Y.; Wong, J. Y. Early Transmission Dynamics in Wuhan, China, of Novel Coronavirus-Infected Pneumonia. *N. Engl. J. Med.* **2020**, *382*, 1199.
(4) Gani, R.; Leach, S. Transmission Potential of Smallpox in Contemporary Populations. *Nature* **2001**, *414* (6865), 748−751.
(5) Nunn, A.; Masud, S.; Krajden, M.; Naus, M.; Jassem, A. N. Diagnostic Yield of Laboratory Methods and Value of Viral Genotyping during an Outbreak of Mumps in a Partially Vaccinated Population in British Columbia, Canada. *J. Clin. Microbiol.* **2018**, *56* (5), 1−8.
(6) Mashazi, P.; Vilakazi, S.; Nyokong, T. Design and Evaluation of an Electrochemical Immunosensor for Measles Serodiagnosis Using Measles-Specific Immunoglobulin G Antibodies. *Talanta* **2013**, *115*, 694−701.
(7) Mashazi, P.; Tetyana, P.; Vilakazi, S.; Nyokong, T. Electrochemical Impedimetric Immunosensor for the Detection of Measles-Specific IgG Antibodies after Measles Infections. *Biosens. Bioelectron.* **2013**, *49*, 32−38.
(8) Gooding, J. J.; Darwish, N. The Rise of Self-Assembled Monolayers for Fabricating Electrochemical Biosensors-an Interfacial Perspective. *Chem. Rec.* **2012**, *12* (1), 92−105.
(9) Willey, T. M.; Vance, A. L.; Van Buuren, T.; Bostedt, C.; Terminello, L. J.; Fadley, C. S. Rapid Degradation of Alkanethiol-Based Self-Assembled Monolayers on Gold in Ambient Laboratory Conditions. *Surf. Sci.* **2005**, *576* (1−3), 188−196.
(10) Crudden, C. M.; Horton, J. H.; Ebralidze, I. I.; Zenkina, O. V.; McLean, A. B.; Drevniok, B.; She, Z.; Kraatz, H.-B.; Mosey, N. J.; Seki, T.; et al. Ultra Stable Self-Assembled Monolayers of N-Heterocyclic Carbenes on Gold. *Nat. Chem.* **2014**, *6* (5), 409−414.
(11) Dejesus, J. F.; Trujillo, M. J.; Camden, J. P.; Jenkins, D. M. N-Heterocyclic Carbenes as a Robust Platform for Surface-Enhanced Raman Spectroscopy. *J. Am. Chem. Soc.* **2018**, *140* (4), 1247−1250.
(12) Li, Z.; Munro, K.; Ebralize, I. I.; Narouz, M. R.; Padmos, J. D.; Hao, H.; Crudden, C. M.; Horton, J. H. N-Heterocyclic Carbene Self-Assembled Monolayers on Gold as Surface Plasmon Resonance Biosensors. *Langmuir* **2017**, *33* (49), 13936−13944.
(13) Li, Z.; Munro, K.; Narouz, M. R.; Lau, A.; Hao, H.; Crudden, C. M.; Horton, J. H. Self-Assembled N-Heterocyclic Carbene-Based Carboxymethylated Dextran Monolayers on Gold as a Tunable Platform for Designing Affinity-Capture Biosensor Surfaces. *ACS Appl. Mater. Interfaces* **2018**, *10* (21), 17560−17570.
(14) Li, Z.; Narouz, M. R.; Munro, K.; Hao, B.; Crudden, C. M.; Horton, J. H.; Hao, H. Carboxymethylated Dextran-Modified N-Heterocyclic Carbene Self-Assembled Monolayers on Gold for Use in Surface Plasmon Resonance Biosensing. *ACS Appl. Mater. Interfaces* **2017**, *9* (45), 39223−39234.
(15) Ndombo, P. K.; Ndze, V. N.; Mbarga, F. D.; Anderson, R.; Acho, A.; Ebua Chia, J.; Njamnshi, A. K.; Rota, P. A.; Waku-Kouomou, D. Molecular Characterisation of Measles Virus Strains among Refugees from Central African Republic in Cameroon in 2014. *Epidemiol. Infect.* **2018**, *146* (3), 319−323.
(16) Salorinne, K.; Man, R. W. Y.; Li, C. H.; Taki, M.; Nambo, M.; Crudden, C. M. Water-Soluble N-Heterocyclic Carbene-Protected Gold Nanoparticles: Size-Controlled Synthesis, Stability, and Optical Properties. *Angew. Chem., Int. Ed.* **2017**, *56* (22), 6198−6202.
(17) Porter, M. D.; Bright, T. B.; Allara, D. L.; Chidsey, C. E. D. Spontaneously Organized Molecular Assemblies. 4. Structural Characterization of n-Alkyl Thiol Monolayers on Gold by Optical Ellipsometry, Infrared Spetcroscopy, and Electrochemistry. *J. Am. Chem. Soc.* **1987**, *109*, 3559−3568.
(18) Mayall, R. M.; Renaud-Young, M.; Chan, N. W. C.; Birss, V. I. An Electrochemical Lipopolysaccharide Sensor Based on an Immobilized Toll-Like Receptor-4. *Biosens. Bioelectron.* **2017**, *87*, 794−801.
(19) Mayall, R. M.; Renaud-Young, M.; Gawron, E.; Luong, S.; Creager, S.; Birss, V. I. Enhanced Signal Amplification in a Toll-like Receptor-4 Biosensor Utilizing Ferrocene-Terminated Mixed Monolayers. *ACS Sensors* **2019**, *4*, 143−151.
(20) Mayall, R. M.; Birss, V. I.; Creager, S. E. Digital Simulation and Experimental Validation of Redox Mediation at an Electroactive Monolayer-Coated Electrode. *J. Electrochem. Soc.* **2020**, *167*, 046512.
(21) Laksono, B. M.; de Vries, R. D.; McQuaid, S.; Duprex, W. P.; de Swart, R. L. Measles Virus Host Invasion and Pathogenesis. *Viruses* **2016**, *8* (8), 210.
(22) Alfson, K. J.; Avena, L. E.; Beadles, M. W.; Staples, H.; Nunneley, J. W.; Ticer, A.; Dick, E. J.; Owston, M. A.; Reed, C.; Patterson, J. L.; et al. Particle-to-PFU Ratio of Ebola Virus Influences Disease Course and Survival in Cynomolgus Macaques. *J. Virol.* **2015**, *89* (13), 6773−6781.
(23) Numazaki, Y.; Karzon, D. T. Density Separable Fractions during Growth of Measles Virus. *J. Immunol.* **1966**, *97* (4), 458−469.
(24) Schaefer, J. V.; Sedlák, E.; Kast, F.; Nemergut, M.; Plückthun, A. Modification of the Kinetic Stability of Immunoglobulin G by Solvent Additives. *MAbs* **2018**, *10* (4), 607−623.